

A Local-Circulation Model for Darrieus Vertical-Axis Wind Turbines

Bernard Massé*

Institut de Recherche d'Hydro-Québec, Québec, Canada

A new computational model for the aerodynamics of the vertical-axis wind turbine is presented. Based on the local-circulation method generalized for curved blades, combined with a wake model for the vertical-axis wind turbine, it differs markedly from current models based on variations in the streamtube momentum and vortex models using the lifting-line theory. A computer code has been developed to calculate the loads and performance of the Darrieus vertical-axis wind turbine. The results show good agreement with experimental data and compare well with other methods.

Introduction

THE computer codes currently used to calculate the loads and performance of vertical-axis wind turbines can be divided into two categories according to whether they are based on momentum or vortex theory. In each case, the problem to be solved consists of evaluating the velocity field inside the rotor and calculating the blade forces using lift and drag data obtained from wind tunnel measurements. Momentum models, also called streamtube models, calculate the induced velocity at the rotor blade by equating the loss of momentum in a streamtube to the forces acting on the blades. Templin's single-streamtube model¹ stated the basis of this theory and has been followed by several refinements to the multiple-streamtube² and double-actuator disk models including flow expansion.³ The vortex models are subdivided according to whether the wake is considered fixed or free. The fixed-wake model developed by Holme,⁴ and the more complex free-wake approach by Strickland,⁵ determine the forces using the Kutta-Joukowski law, the airfoil section lift, and the circulation.

The main assumptions underlying the momentum models are that each streamtube is aerodynamically independent of the others and is fixed in both location and time. They use average values for the inside of each tube and consider the flow as being steady. The free-wake vortex model can theoretically be used to introduce unsteady aerodynamics and operate in the transient state, but even in the steady state it requires a large amount of computer time and is known to have convergence problems. Therefore, a new approach was required to calculate the loads on the blades of the Darrieus wind turbine that would not have the inherent limitations of the momentum models or be hampered by the excessive computer times and convergence problems noted for the vortex model. One such approach has been presented by Azuma and Kimura⁶ based on the local-circulation method. Independently, the present author has developed a model that combines the local-circulation method with a fixed-wake model based on Holme's equations. It results in a new formulation that offers many advantages over momentum models, avoids convergence problems, and requires much less computer time than either the vortex model or Azuma and Kimura's model.

The first part of this paper describes the rotor model, including the basic equations, blade representation, bound vortex-induced velocities, and blade force calculation. The next part is related to the wake model used in conjunction with the rotor model. Holme's⁴ equations have been modified to include the blade curvature and a simple wake model is derived. A computer program, MCL, based on the new model, is briefly described and analytical results are compared to experimental data and other aerodynamic codes.

Rotor Model

A local-circulation method has been proposed by Azuma and Kawachi⁷ for helicopter rotors. The original method, the so-called momentum theory, was developed to calculate the dynamic loads of a helicopter rotor. In that version, the induced velocity was assumed normal to the plane of the rotor but for propellers and wind turbines this assumption is not valid, while in addition the inflow angle may vary substantially along the span. The method was consequently reformulated as the "local-circulation method"⁸. However, to be able to use this method for the Darrieus wind turbine, the equations must be modified to take account of the blade curvature. The real blade is represented by superposing imaginary blades. The induced velocities are calculated using the Biot-Savart law for the curved blade and the forces are estimated using two-dimensional airfoil data.

Basic Equation

The lift about a blade element is related to the circulation $\Gamma(y)$ by the Kutta-Joukowski law, but can also be expressed in terms of the lift coefficient C_L and the square of the velocity relative to the blade V_r^2 . Equating these two expressions for the lift yields an equation that relates the local circulation, the lift coefficient, and the relative velocity as follows:

$$\Gamma(y) = \frac{1}{2} C_L c V_r \quad (1)$$

where c is the chord of the blade element. The lift coefficient is a nonlinear function of the effective angle of attack α_e for angles larger than the stall angle, and C_L is also a function of the Reynolds number. The relative-velocity term includes the induced velocities produced by the other blade elements and the turbine wake. Equation (1) is solved for each blade element and implies an interaction process because of the nonlinearity of the expression.

Received Jan. 31, 1985; revision received Oct. 4, 1985. Copyright © American Institute of Aeronautics and Astronautics, Inc., 1985. All rights reserved.

*Research Scientist; also Ph.D. Student, Sherbrooke University, Québec, Canada.

Blade Decomposition

In the local-circulation method, the real blade with an arbitrary circulation distribution is represented by superposing imaginary blades of different spans with an elliptical circulation distribution. For the Darrieus wind turbine, an asymmetrical arrangement was chosen (as shown in Fig. 1) to allow asymmetrical airloading (e.g., wind shear due to the atmospheric boundary-layer wind profile) to be included. The circulation at a given point on the blade is the sum of the circulations of the imaginary blades at the same ordinate,

$$\Gamma(y) = \sum_{i=1}^k \Delta\Gamma_i(y) \quad (2)$$

where k is the number of imaginary blades at the given point and $\Delta\Gamma_i(y)$ the circulation on the i th imaginary blade at the ordinate y . The distribution of circulation on this blade being elliptical,

$$\Delta\Gamma_i(y) = \Delta\Gamma_{0i} \sqrt{1 - (y/s)^2} \quad (3)$$

where $\Delta\Gamma_{0i}$ is the circulation at the center of the i th blade, at $\ell=0$. The $\Delta\Gamma_{0i}$ are the unknown values and the i th control point on the real blade is used to evaluate the i th $\Delta\Gamma_{0i}$, since the number of imaginary blades is determined by the number of control points. The solution of Eq. (1) is an iteration over $\Delta\Gamma_{0i}$ for each control point and the solution along the blade is a recurrent process.

Induced Velocity

The local-circulation method has been developed for straight blades⁸ so that when applied to Azuma and Kimura's⁶ vertical-axis wind turbine the curved blade had to be approximated by a polygonal blade consisting of a succession of straight lines inside the curved blade. The present model takes account of the true shape of the blade and uses a curved-blade coordinate system to generalize the equations so as to include the effect of blade curvature. The straight-blade solution is a subset of this more general model.

Figure 2 illustrates a curved-blade segment of a Darrieus wind turbine and shows the coordinate system used to calculate the induced velocity. A vortex sheet is formed behind the blade due to the circulation distribution along the blade span. At a location ℓ' along the blade, the intensity $d\Gamma(\ell')$ is determined by the slope of the distribution $d\Gamma(\ell') = [d\Gamma(\ell')/d\ell'] d\ell'$. Using the assumption that the vortex $d\Gamma(\ell')$ travels in a straight line along the i' axis and applying the Biot-Savart law, the induced velocity at a position ℓ on the blade is calculated by

$$\vec{v} = -\frac{1}{4\pi} \int_{-s}^s \frac{1}{Z_{\ell,\ell'}} \frac{d\Gamma(\ell')}{d\ell'} d\ell' \quad (4)$$

The angle β' (Fig. 2) is defined between the j' axis and the rotation axis, and the three components of the induced velocity are given by

$$\begin{bmatrix} v_x \\ v_y \\ v_z \end{bmatrix} = \begin{bmatrix} \cos(\phi' - \phi) & \sin(\phi' - \phi)\sin(\delta - \beta') & -\sin(\phi' - \phi)\cos(\delta - \beta') \\ 0 & \cos(\delta - \beta') & \sin(\delta - \beta') \\ \sin(\phi' - \phi) & -\cos(\phi' - \phi)\sin(\delta - \beta') & \cos(\phi' - \phi)\cos(\delta - \beta') \end{bmatrix} \begin{bmatrix} 0 \\ 0 \\ v \end{bmatrix} \quad (5)$$

so that the perpendicular component of the induced velocity is

$$v_z = v \cos\psi; \quad \cos\psi = \cos(\phi' - \phi) \cos(\delta - \beta') \quad (6)$$

The components in the flow direction and along the j axis are, respectively,

$$v_x = -v_z \tan(\phi' - \phi) \quad \text{and} \quad v_y = v \sin(\delta - \beta') \quad (7)$$

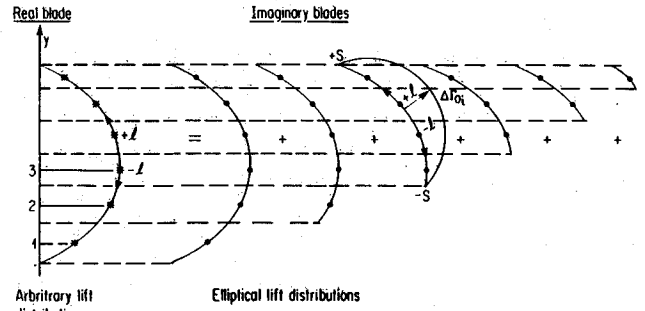


Fig. 1 Decomposition of the real blade into imaginary blades.

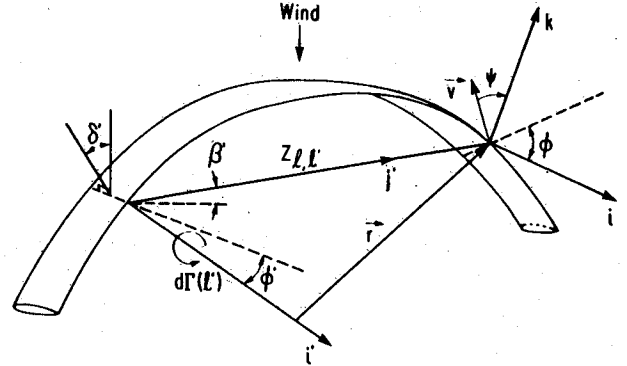


Fig. 2 Induced velocity on a curved blade.

In Eq. (6), $\cos\psi$ can be written as

$$\begin{aligned} \cos\psi &= 1 - 2 \sin^2 \left(\frac{\delta - \beta'}{2} \right) - 2 \sin^2 \left(\frac{\phi' - \phi}{2} \right) \\ &\times \left[1 - 2 \sin^2 \left(\frac{\delta - \beta'}{2} \right) \right] \end{aligned} \quad (8)$$

Substituting this expression into Eqs. (6) and (4), the induced velocity perpendicular to the inflow at a location ℓ along the curved blade is expressed as

$$v_z = -\frac{1}{4\pi} \int_{-s}^s \frac{\cos\psi}{Z_{\ell,\ell'}} \frac{d\Gamma(\ell')}{d\ell'} d\ell' = \frac{-1}{4\pi} (I_1 + I_2) \quad (9)$$

where

$$I_1 = \int_{-s}^s \frac{1 - 2 \sin^2 [(\delta - \beta')/2]}{Z_{\ell,\ell'}} \frac{d\Gamma(\ell')}{d\ell'} d\ell' \quad (10)$$

and

$$I_2 = - \int_{-s}^s \frac{2 \sin^2 [(\phi' - \phi/2)] [1 - 2 \sin^2(\delta - \beta')/2]}{Z_{\ell, \ell'}} \times \frac{d\Gamma(\ell')}{d\ell'} d\ell' \quad (11)$$

Equation (9) can be used to calculate the perpendicular component of the induced velocity produced by the vortex sheet and for an arbitrary circulation distribution, at any location along the blade.

For a blade with an elliptic distribution, Eq. (9) becomes

$$\Delta v_z = - \frac{\Delta \Gamma_0}{4\pi s} \int_{-s}^s \frac{\cos \psi}{Z_{\ell, \ell'}} \frac{\ell'}{\sqrt{s^2 - \ell'^2}} d\ell' \quad (12)$$

This integral is singular when $\ell = \ell'$ and when $\ell'^2 = s^2$. The singularities at the bounds are eliminated with a suitable change of variables and the singularity at $Z_{\ell, \ell'} = 0$ calls for a solution through the Cauchy principal value. When the integral is divided into the sum of two integrals I_1 and I_2 , Eqs. (10) and (11), only the first integral [Eq. (10)] has the singularity and is a function of the geometry only. In I_2 , when $\ell = \ell'$, ϕ is equal to ϕ' and the integrand tends to zero, avoiding the singularity problem. The integral of Eq. (11) is a function of the geometry and also of the twisted inflow along the span. The term $Z_{\ell, \ell'}$ depends on the blade geometry, and its expression is specific to the wind turbine considered. It can be shown that for a straight blade, $\delta = \beta' = 0$ and Eqs. (10) and (11) reduce to the equation given in Ref. 8.

Force Calculation

The induced velocity normal to the flow on the real blade is the sum of the normal induced velocities on the k imaginary blades at the same control-point location:

$$v_z(y) = \sum_{i=1}^k \Delta v_{zi} \quad (13)$$

The velocity relative to the blade is designated V_r and the blade section, including the induced velocity and the corresponding lift and drag, is shown schematically in Fig. 3. The induced angle α_i is defined as

$$\alpha_i \approx V_{zi}/V_r \quad (14)$$

$V_{zi} \ll V_r$ and $\alpha_i \approx \sin \alpha_i \approx \tan \alpha_i$. This change in the angle of attack is responsible for a reduction in the lift, $dR \cos \alpha_i$ for a blade of finite span. The effective angle of attack, $\alpha_e = \phi - \alpha_i$, is used to calculate the lift and drag coefficients from two-dimensional wind tunnel data and the induced drag, $dL(V_{zi}/V_r)$, is added to the profile drag. Most of the aerodynamic codes used for the Darrieus wind turbine neglect the induced angle of attack produced by the bound vortex along the span and make direct use of the geometric angle of attack ϕ calculated only in terms of the velocity induced by the wake. The present model introduces an additional degree of accuracy by considering the blade self-interference, a three-dimensional effect that has been investigated by comparison with experimental data and results from other aerodynamic codes. The importance of the angle induced by the bound vortex is discussed in a later section.

Wake Model

The circulation at a given location along the blade, $\Gamma(y)$, is a function of the circumferential position θ of the rotor. As the blade moves along the circumference with a certain angular variation, $d\theta$, a vortex $-d\Gamma(\theta)$ leaves the blade and follows the general flow. A wake is then formed by the

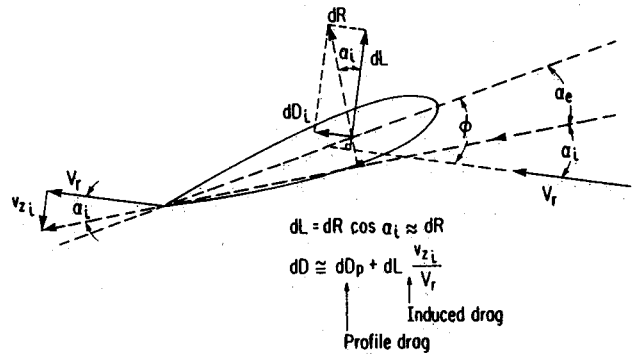


Fig. 3 Induced angle of attack and induced drag.

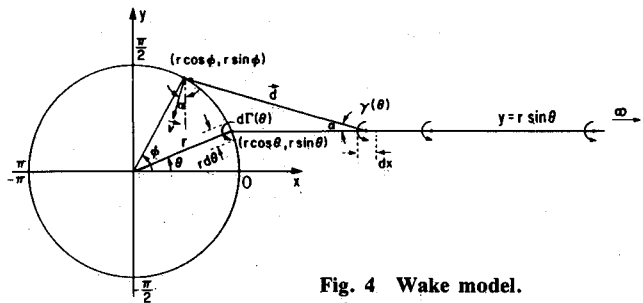


Fig. 4 Wake model.

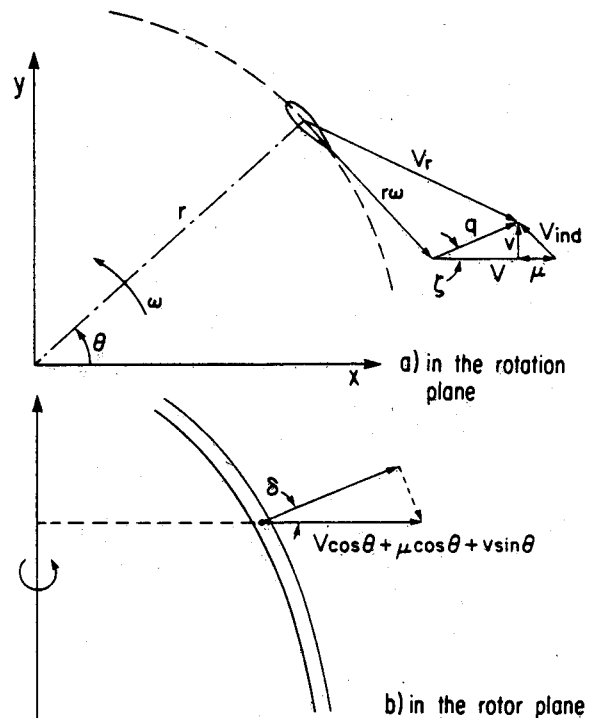


Fig. 5 Velocity diagrams.

blades moving upstream and more vortices are added to it by the blades moving downstream. The model proposed by Holme for straight blades in a steady flow⁴ has shown that one-half of the wind velocity decreased within the rotor, an observation that has been incorporated in several momentum theories. For the present model, a simple solution is obtained for the wake that takes into account upwind and downwind interference and wake expansion. The wake equations are derived from Holme's model but extended for curved blades and use a consistent assumption for the radial velocity function and its derivative.

Basic Equations

The geometric shape of the vortex filaments leaving the blades is very complex. A simpler model can be developed assuming straight lines in the flow direction. The transverse component of vorticity inside the rotor is then neglected, although this limits the validity of the model to cases where the perturbations are small compared to the main flow. Figure 4 represents such a vortex filament and the velocity induced by the vortex γ is

$$dv = -\frac{\gamma(\theta)}{2\pi |d|} \quad (15)$$

The velocity induced by the whole vortex filament is obtained by integrating along the filament:

$$v_x = -\frac{\gamma(\theta)}{2\pi} \int_{x=r\cos\theta}^{\infty} \frac{r\sin\theta - r\sin\phi}{(x-r\cos\phi)^2 + (r\sin\theta - r\sin\phi)^2} dx \quad (16)$$

$$v_y = -\frac{\gamma(\theta)}{2\pi} \int_{x=r\cos\theta}^{\infty} \frac{x - r\cos\phi}{(x-r\cos\phi)^2 + (r\sin\theta - r\sin\phi)^2} dx \quad (17)$$

The solutions of the preceding integrals are

$$v_x = -\frac{\gamma(\theta)}{2\pi} K(\theta, \phi) \quad (18)$$

where

$$K(\theta, \phi) = \tan^{-1} \frac{\cos\phi - \cos\theta}{\sin\phi - \sin\theta} - \frac{\pi}{2} \frac{\sin\phi - \sin\theta}{|\sin\phi - \sin\theta|}$$

$$v_y = -\frac{\gamma(\theta)}{4\pi} \lim_{x \rightarrow \infty} \ln \left(\frac{\chi^2 + h^2}{a^2 + h^2} \right) \quad (19)$$

where

$$\chi = x - r\cos\phi$$

$$a = r\cos\phi - r\cos\theta$$

$$h = r\sin\phi - r\sin\theta$$

The intensity of the vortex filament is written as

$$\gamma(\theta) = -\frac{r\omega}{q(\theta)} \frac{\partial \Gamma(\theta)}{\partial \theta} d\theta \quad (20)$$

where $q(\theta)$ is the velocity of the main flow at a position θ on the circle. Defining the induced velocity along the x and y axes produced by all of the wake filaments as u and v , respectively (Fig. 4), the following integrals are obtained:

$$u(\phi) = \frac{1}{2\pi} \int_{-\pi}^{\pi} \gamma(\theta) K(\theta, \phi) d\theta \quad (21)$$

$$v(\phi) = \frac{1}{4\pi} \int_{-\pi}^{\pi} \gamma(\theta) \lim_{x \rightarrow \infty} \ln \left(\frac{\chi^2 + h^2}{a^2 + h^2} \right) d\theta \quad (22)$$

Equations (20-22) constitute the basic wake model produced by the free vortex and are valid for weak perturbations, which means that the validity of the model is questionable at high tip-speed ratios.

Curved-Blade Model

To solve Eqs. (21) and (22) and obtain a direct solution, Holme used the following equation:

$$q_r(\theta) = Vf(\theta) \quad (23)$$

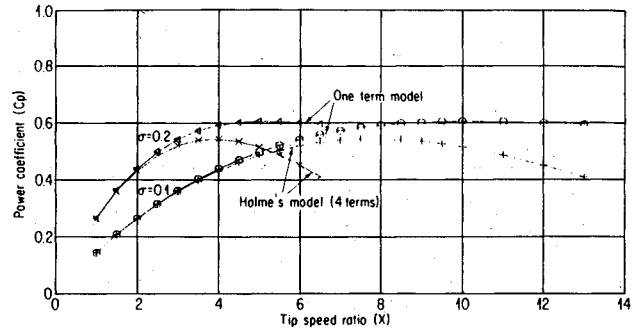


Fig. 6 Power coefficients in nonviscous flow.

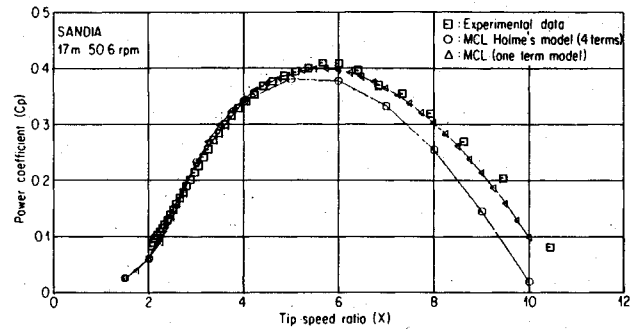


Fig. 7 Effect of the wake model.

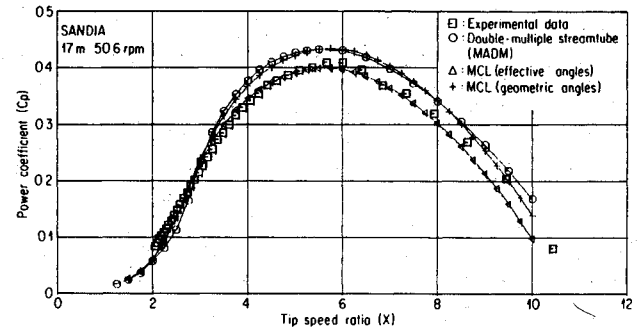


Fig. 8 Effect of the induced angle from the bound vortex.

which relates the radial component of the main flow, $q_r(\theta)$, to the product of the undisturbed flow, V , and a function $f(\theta)$ which can be expressed as a Fourier series,

$$f(\theta) = \sum_{n=1}^{\infty} (a_n \cos n\theta + b_n \sin n\theta) \quad (24)$$

The blade curvature is introduced using the angle between the normal to the blade and the rotation plane (Fig. 5) so that:

$$q_r(\theta) = Vf(\theta) \cos\delta \quad (25)$$

Using this equation instead of Eq. (23) and a development similar to that described in Ref. 4, the coefficients of the Fourier series can be evaluated as

$$a_1 \frac{(1 + \lambda^2 \cos\delta)}{\cos\delta} = 1 - \lambda \left[\frac{1}{2} (A_0 + A_2) \right] \quad (26)$$

$$a_n = -\lambda a_{n-1} \cos\delta, \quad n=2,4,6,\dots$$

$$a_n \frac{(1 + \lambda^2 \cos\delta)}{\cos\delta} = -\lambda \left[\frac{1}{2} (A_{n-1} + A_{n+1}) \right], \quad n=3,5,7,\dots$$

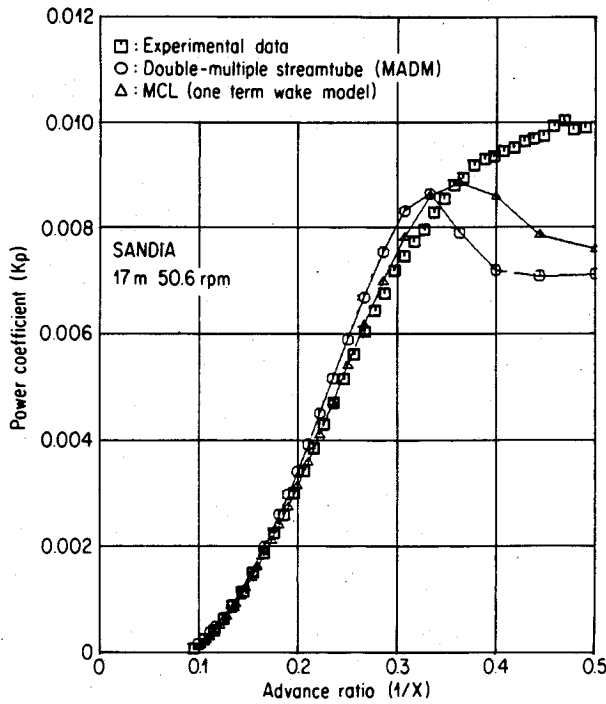


Fig. 9 Power coefficient.

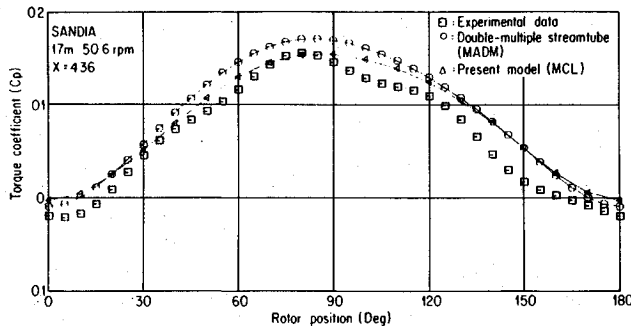


Fig. 10 Aerodynamic torque.

where

$$A_n = \frac{8}{\pi} (-1)^n \sum_{m=1}^{\infty} \frac{(2m-1)(-1)^m a_{2m-1}}{n^2 - (2m-1)^2}, \quad n=0,2,4,\dots$$

$$= 2a_n, \quad n=1,3,5,\dots$$

The b_n coefficients referred to in Ref. 4 are equal to zero, only the free vortex being of interest, and λ is the vortex filament intensity parameter based on an average flow velocity through the turbine, \bar{q} . This average velocity is estimated using the mass flow coefficient C_m calculated from the streamlines, which can be expressed as a function of $f(\theta)^4$. The calculation of λ and the coefficient of $f(\theta)$ is an iterative process.

One-Term Model

It can be demonstrated that the assumption of a constant velocity, \bar{q} , in the turbine allows the integration of Eqs. (21) and (22). Using

$$\gamma(\theta) = -2V\sigma\cos\delta \frac{r\omega}{q(\theta)} \frac{\partial f(\theta)}{\partial \theta} \quad (27)$$

integrals (21) and (22) can be written in the following form:

$$\frac{u(\theta)}{V} = -\sigma \frac{r\omega}{V} \frac{\cos\delta}{\pi} \int_{-\pi}^{\pi} K(\theta, \phi) \frac{f'(\phi)}{f(\phi)} \cos\phi d\phi \quad (28)$$

$$\frac{v(\theta)}{V} = -\sigma \frac{r\omega}{V} \frac{\cos\delta}{2\pi} \times \int_{-\pi}^{\pi} \lim_{X \rightarrow \infty} \ln \left(\frac{\chi^2 + h^2}{a^2 + h^2} \right) \frac{f'(\theta)}{f(\theta)} \cos\phi d\phi \quad (29)$$

In the case of the wake model for the Darrieus turbine, $f(\phi)$ is a Fourier series in cosine and $f'(\phi)$ is its derivative. Holme's assumption can be expressed as $f(\phi) = \bar{q}\cos\phi/V = C_m\cos\phi$ and the two equations above can be integrated. Unfortunately, the solution obtained implies that the function $f(\phi)$ is of the form $f(\phi) = a\cos\phi$ and that its derivative $f'(\phi)$ retains all of the terms from the Fourier series. To avoid this inconsistency, it must be assumed that $f'(\phi) = -a\sin\phi$ and the integrals then become

$$\frac{u(\theta)}{V} = \frac{\sigma X}{\pi} \cos\delta \int_{-\pi}^{\pi} K(\theta, \phi) \sin\phi d\phi \quad (30)$$

$$\frac{v(\theta)}{V} = -\frac{\sigma X}{2\pi} \cos\delta \int_{-\pi}^{\pi} \lim_{X \rightarrow \infty} \ln \left(\frac{\chi^2 + h^2}{a^2 + h^2} \right) \sin\phi d\phi \quad (31)$$

which can easily be solved to generate the simple expressions for induced velocities from the wake as

$$\frac{u(\theta)}{V} = \sigma X \cos\delta \left[\cos\theta - \left(1 + \frac{\cos\theta}{|\cos\theta|} \right) 2\cos\theta \right] \quad (32)$$

or

$$= \sigma X \cos\theta \cos\delta \quad \text{upstream}$$

$$= -3\sigma X \cos\theta \cos\delta \quad \text{downstream}$$

and

$$\frac{v(\theta)}{V} = \sigma X \sin\theta \cos\delta \quad (33)$$

This simple solution is obtained using the same number of terms in $f(\phi)$ and $f'(\phi)$ and is not obtained from iteration on λ as in Holme's model. Furthermore, for an ideal turbine, $C_D = 0$, and assuming a lift slope of 2π , the maximum power coefficient, $C_{p_{\max}}$, is 0.606 (as compared to 0.545 from Holme⁴) and is close to the classical Betz's limit (0.593). Loth and McCoy⁹ have shown a maximum performance coefficient of 0.640 for two uniformly loaded disks in series but also a $C_{p_{\max}}$ of 0.617 for cosine-loaded semi-cylindrical actuators in series and a value of 0.610 for a straight-bladed Darrieus rotor which is close to 0.606 obtained with the present model. Holme's model, based on four terms in the derivative, $f'(\phi)$, and Eqs. (32) and (33), was used to calculate the power coefficient for an ideal straight-blade turbine. Results are shown in Fig. 6 for two different solidities. The difference between the models is significant close to the maximum power coefficient and increases with the tip-speed ratio. The two wake models are combined with the rotor model developed in the preceding sections and compared to experimental data.

Results and Discussion

A computer code has been derived using the rotor and wake models developed for curved blades as used for the Darrieus wind turbine. Calculations on the Sandia 17-m wind turbine¹⁰ (Fig. 7) confirm the validity of the new method. As expected (see discussion in the preceding sec-

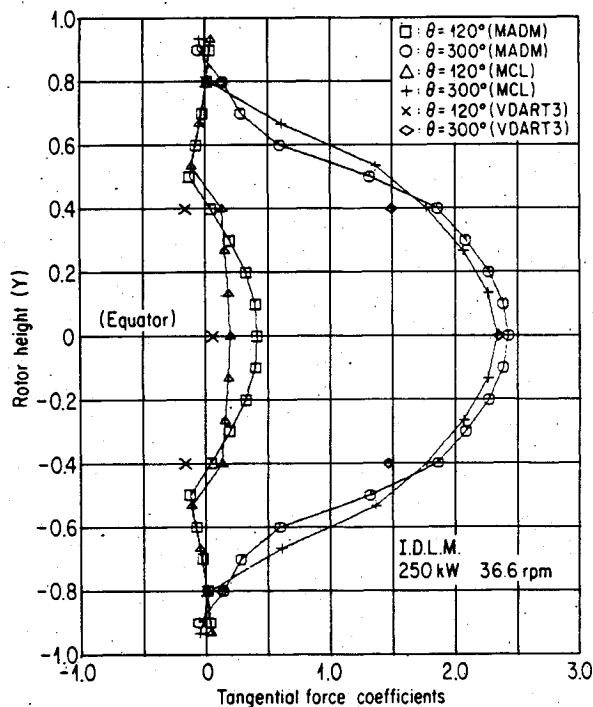


Fig. 11 Tangential force distribution along the blade, $X=2.3$.

tion), the one-term wake model gives good results compared to experimental data, whereas Holme's model underpredicts the power coefficient at maximum and high tip-speed ratios. The one-term wake model has the advantage of being simpler and more accurate and is used for the rest of the calculations. Figure 8 shows a comparison with the double-multiple streamtube model.¹¹ For that purpose, the present code (MCL) was run with and without the calculation of the velocities induced by the bound vortex on the curved blade. The results show that when this effect is ignored the solution obtained with MCL is similar to that obtained with the double-actuator-disk momentum model. When the induced angle and corresponding induced drag are calculated, the results show a better fit with the experimental data. The present rotor model, which considers the blade to be curved and of finite span, gives more accurate predictions than the momentum models, which consider each position along the rotor height as being independent of the others. The same improvement is also shown on the K_p curve (Fig. 9), which is similar in shape to the power curve of the turbine and the MCL results are closer to the experimental data than the double-multiple streamtube. Dynamic stall is intentionally ignored in the models in order to compare the basic methods, which is why the stall region is underpredicted by both methods.

The aerodynamic torque on the Sandia 17-m wind turbine has been measured by McNerney.¹² The dynamic stall effect is small at a tip-speed ratio of 4.36; this condition is used to compare the present method with experimental data in Fig. 10. Also shown in this figure is the calculation with the double-multiple streamtube. Again, good agreement with experimental data is obtained.

The load distribution along the blades in the tangential and normal directions is calculated with MCL for a given rotor position and compared to the double-multiple streamtube and the vortex models. The turbine is the Magdalen Islands vertical-axis wind turbine at 36.6 rpm.

The vortex model was used without considering the dynamic effects in order to compare the models on the same basis. To obtain an acceptable computer time, the blade is approximated by five straight elements, as is normal with this code. The results of the three codes in Figs. 11 and 12

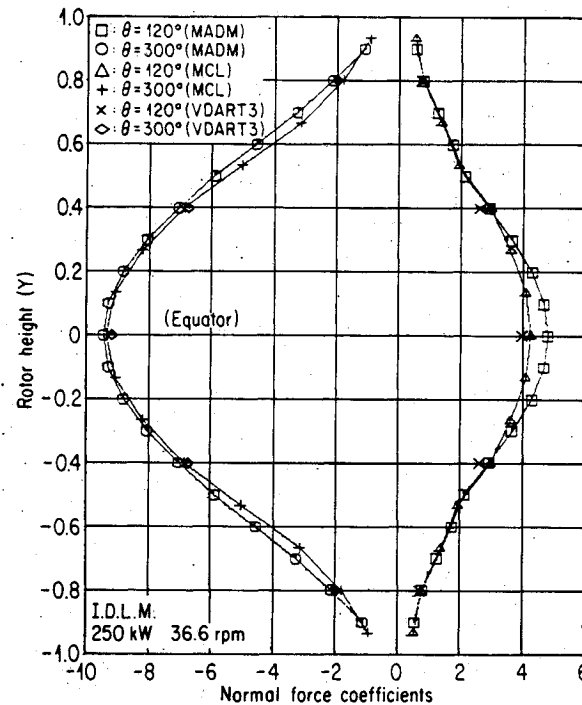


Fig. 12 Normal force distribution along the blade, $X=2.3$.

show good agreement with MCL and the vortex model at the equator, indicating that generally speaking MCL is valid compared to other aerodynamic codes. Unfortunately, no experimental data are available to determine which code gives better results.

Different runs of the present model, the double-multiple streamtube and vortex models, on the same computer reveal that the computing times are of the same order of magnitude for the first two but much longer for the vortex model, which is known to require a great deal of computer time and has to converge to the solution. The computer time of Azuma and Kimura's model is reported in Ref. 6 as being 3 min, using a FACOM-M-200 computer to complete the calculation for one tip-speed ratio with a 15-deg azimuthal step. The computer used for MCL is an IBM-3081 K, which is slightly slower than the FACOM. Furthermore, MCL uses a 10-deg steps on the azimuth. To give an order of magnitude of the difference in the computing time, MCL calculates one tip-speed ratio in about one-hundredth of a minute, which is 300 times faster than the model of Ref. 6. The way the rotor model has been developed and the simple wake model derived from Holme's equations results in a fairly accurate and efficient tool for Darrieus wind-turbine aerodynamic calculation.

Conclusions

A new model for the Darrieus rotor aerodynamic calculation has been derived from the local-circulation method extended to curved blades. The effect of blade curvature has been included in Holme's wake equations and a simple formulation for wake-induced velocities is obtained. The new set of equations for the rotor and the wake is used in a computer code, MCL, and the results indicate good agreement with experimental data on the Sandia 17-m wind turbine and compare favorably with other methods. The new model is fairly accurate, uses computing time efficiently, and has no convergence problems.

References

- Templin, R. J., "Aerodynamic Performance Theory for the NRC Vertical-Axis Wind Turbine," NRC Canada, LTR-LA-160, 1974.

²Strickland, J. H., "The Darrieus Turbine: A Performance Prediction Model Using Multiple Streamtubes," Sandia National Laboratory, Albuquerque, NM, SAND 75-0431, 1975.

³Read, S. and Sharpe, D. J., "An Extended Multiple Streamtube Theory for Vertical-Axis Wind Turbines," *Proceedings of the 2nd BWEA Wind Energy Workshop*, Cranfield, U.K., 1980, pp. 65-72.

⁴Holme, O., "A Contribution to the Aerodynamic Theory of the Vertical-Axis Wind Turbine," International Symposium on Wind Energy Systems, Cambridge, England, Paper C4, Sept. 1976.

⁵Strickland, J. H., Smith, T., and Sun, K., "A Vortex Model of the Darrieus Turbine: An Analytical and Experimental Study," Sandia National Laboratory, SAND 81-7017, June 1981.

⁶Azuma, A. and Kimura, S., "A Method of Calculation on the Airloading of Vertical-Axis Wind Turbines," *Proceedings of the 18th Intersociety Energy Conversion Engineering Conference*, Orlando, FL, Aug. 1983.

⁷Azuma, A. and Kawachi, K., "Local Momentum Theory and Its Application to the Rotary Wing," AIAA Paper 75-865, June 1975.

⁸Azuma, A., Nasu, K., and Kayashi, T., "An Extension of the Local Momentum Theory to Rotors Operating in a Twisted Flow Field," *Vertica*, Vol. 7, No. 1, 1983, pp. 45-49.

⁹Loth, J. L. and McCoy, H., "Optimization of Darrieus Turbines with an Upwind and Downwind Momentum Model," *Journal of Energy*, Vol. 7, No. 4, 1983, pp. 313-318.

¹⁰Klimas, P. C., "Vertical-Axis Wind Turbine Aerodynamic Performance Prediction Methods," *Proceedings of the Vertical-Axis Wind Turbine (VAWT) Design Technology Seminar for Industry*, Albuquerque, NM, April 1980, pp. 215-232.

¹¹Massé, B., "Description de deux programmes d'ordinateur pour le calcul des performances et des charges aérodynamiques pour les éoliennes à axe vertical," Institut de Recherche d'Hydro-Québec, IREQ-2379, July 1981.

¹²McNerney, G. M., "Accelerometer Measurements of Aerodynamic Torque on the DOE/Sandia 17-m Vertical Axis Wind Turbine," Sandia National Laboratory, Albuquerque, NM, SAND 80-2776, 1980.

From the AIAA Progress in Astronautics and Aeronautics Series...

LIQUID-METAL FLOWS AND MAGNETOHYDRODYNAMICS—v.84

*Edited by H. Branover, Ben-Gurion University of the Negev
P.S. Lykoudis, Purdue University
A. Yakhot, Ben-Gurion University of the Negev*

Liquid-metal flows influenced by external magnetic fields manifest some very unusual phenomena, highly interesting scientifically to those usually concerned with conventional fluid mechanics. As examples, such magnetohydrodynamic flows may exhibit M-shaped velocity profiles in uniform straight ducts, strongly anisotropic and almost two-dimensional turbulence, many-fold amplified or many-fold reduced wall friction, depending on the direction of the magnetic field, and unusual heat-transfer properties, among other peculiarities. These phenomena must be considered by the fluid mechanician concerned with the application of liquid-metal flows in partial systems. Among such applications are the generation of electric power in MHD systems, the electromagnetic control of liquid-metal cooling systems, and the control of liquid metals during the production of the metal castings. The unfortunate dearth of textbook literature in this rapidly developing field of fluid dynamics and its applications makes this collection of original papers, drawn from a worldwide community of scientists and engineers, especially useful.

Published in 1983, 454 pp., 6×9, illus., \$25.00 Mem., \$55.00 List

TO ORDER WRITE: Publications Order Dept., AIAA, 1633 Broadway, New York, N.Y. 10019